NANO LETTERS

LETTER

pubs.acs.org/NanoLett

On-Nanowire Spatial Band Gap Design for White Light Emission

Zongyin Yang,[‡] Jinyou Xu,[†] Pan Wang,[‡] Xiujuan Zhuang,[†] Anlian Pan,*[,†] and Limin Tong*[,‡]

[†]College of Physics and Microelectronics Science, Key Laboratory for Micro-Nano Physics and Technology of Hunan Province, Hunan University, Changsha 410082, China

[‡]State Key Laboratory of Modern Optical Instrumentation, Department of Optical Engineering, Zhejiang University, Hangzhou 310027, China

Supporting Information

ABSTRACT: We demonstrated a substrate-moving vapor−liquid−solid (VLS) route for growing composition gradient ZnCdSSe alloy nanowires. Relying on temperature-selected composition deposition along their lengths, single tricolor ZnCdSSe alloy nanowires with engineerable band gap covering the entire visible range were obtained. The photometric property of these tricolor nanowires, which was determined by blue-, green-, and red-color emission intensities, can be in turn controlled by their corresponding emission lengths. More particularly, under carefully selected growth conditions, on-nanowire white light emission has been achieved. Band-gap-engineered semiconductor alloy nanowires demonstrated here may find applications in broad band light absorption and emission devices.

KEYWORDS: Semiconductor nanowire, band gap engineering, tunable photoluminescence, white light emission

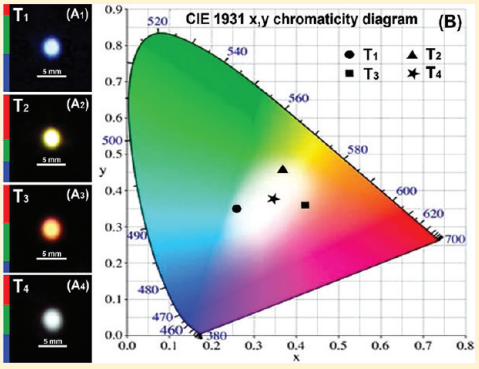

Color controlled solid-state light emitting, especially semiconductor-based solid-state white lighting, has attracted great attention for the higher conversion efficiency and more flexible control of photometric properties compared with the conventional incandescent lighting.[1] White light can be formed by mixing lights of different colors, such as red, green, and blue (RGB). A feasible approach for white lighting is to mix light emitting diodes (LEDs) of proper wavelengths and intensity ratios.[2,3] Although this route has the potential for high luminous efficiency, low color rendering index (CRI) and stability do not make the light aesthetically pleasing. The other approach is to combine the phosphor-based wavelength down-conversion medium with a blue or UV light excitation.[4] This phosphor-based white technology can achieve a good color quality, but its efficiency is severely limited by the inevitable Stokes energy loss which is not incurred in the semiconductor-based white light sources. A major challenge in solid-state lighting research is to achieve rationally designed semiconductor-based light-emitting materials or structures with both reasonable power efficiency and color quality.[3,5]

The emerging nanotechnology has brought a variety of new opportunities for solid-state white lighting research.[6−15] In particular, semiconductor nanostructures, such as semiconductor alloy nanowires, have shown the potential in constructing white lighting sources due to their high quantum efficiency and wide band gap tunability.[16−18] Using the vapor−liquid−solid (VLS) nanowire growth mechanism,[8] the element composition in the grown nanowires can directly be controlled by the corresponding element concentration in the source materials or the precursor vapor,[19−25] and semiconductor alloys with different band gaps can be gradually grown into single wires along their length, through applying an in situ concentration changing of the source reagents during the growth.[13,26−33] These band gap graded semiconductor nanostructures offer the opportunity to design novel white light-emitting materials or structures at microscale from the ground up.

To realize white-light-emitting band gap graded semiconductor nanowires, the most important issue is to get wires with band gap tunability in the entire visible region and have the capability to selectively control the band gap/composition along the wires. Due to the differences in condensation temperatures and growth kinetics during the catalyst-assistant VLS growth, it was observed that alloy nanowires with different alloy compositions could deposit at different positions along the length of the growth tube with a temperature gradient.[34,35] By use of this temperature-selected composition dispersive phenomenon, quarternary ZnCdSSe alloy nanowires with band gap tunability covering the full visible range were grown along the length of a single substrate.[36,37] In this work, based on this temperature-selected composition dispersion, we developed a substrate moving strategy in the VLS process and realized the growth of composition gradient ZnCdSSe alloy nanowires (full-color nanowires), with gradually tunable band gaps covering the entire visible range along the length of the wires. More importantly, the relative length of selected band gap/composition segments along the wires can be controlled during the growth. Using the tricolor (RGB) based white emission principle[2,3] and through careful composition control, we realized the color-controlled nanowire white light emission (tricolor nanowires). Results demonstrated in this work may open new opportunities to realizing nanoscale white light sources for a variety of applications.

Received: October 7, 2011
Published: October 19, 2011

dx.doi.org/10.1021/nl203529h | *Nano Lett.* 2011, 11, 5085–5089

Figure 1a shows the schematic setup for the growth of full-color band gap graded ZnCdSSe alloy nanowires. A horizontal quartz tube (inner diameter 45 mm, length 120 cm) was mounted inside a single-zone furnace. In the tube, an alumina boat with ZnS powder (Alfa Aesar, 99.99% purity) was loaded at the center of the heating zone, and another boat with CdSe powder (Alfa Aesar, 99.995% purity) was placed upstream of the tube with a temperature of about 800 °C. A silicon substrate coated with a 2 nm thick gold film was vertically mounted to a quartz rod driven by a magnet system during the growth. The different colors of the deposition zone (from positions A to B) downstream of the tube indicate the different band gaps/compositions of the corresponding deposited materials (see Figure 1a). The system was flushed with high-purity N_2 for 1 h to eliminate O_2, and the silicon substrate was located at position A before heating. Then the furnace was rapidly heated to 1000 °C with a constant flow of 50 SCCM N_2 under ~15 Torr pressure. Ten minutes later, the silicon substrate was pulled from position A to B by a magnet at a velocity of 5 cm min^{-1}. After 4 min of growth in position B, the furnace was turn off and cooled down to room temperature naturally. Band gap graded full-color ZnCdSSe alloy nanowires were collected on the silicon substrate. The formation process of these full-color wires is schematically shown in Figure 1b.

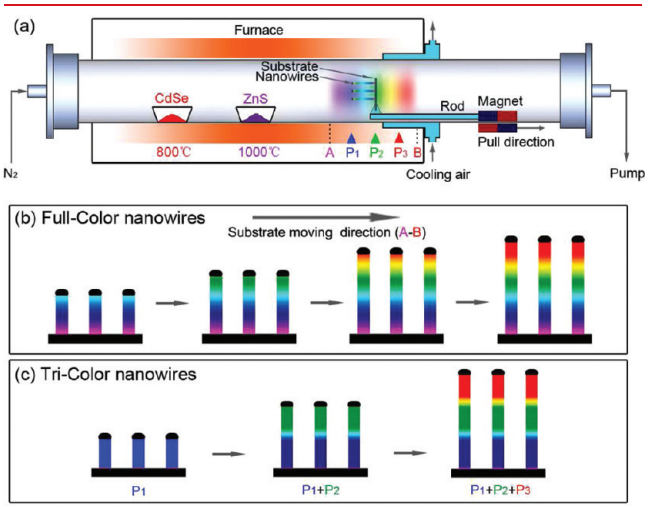

Figure 1. Schematic diagrams of the experimental setup (a) and the growth processes for full-composition (b) and tricolor (c) band gap graded ZnCdSSe nanowires, respectively.

The morphology of the as-grown band gap graded full-color nanowires was characterized by scanning electron microscopy (SEM) and transmission electron microscopy (TEM), as shown in panels a and b of Figure 2, respectively, which show that these graded wires have a uniform diameter of ~80 nm and a length up to ~30 μm. The EDX analysis of a representative single wire indicates that any detected points along the length are composed of Zn, Cd, S, and Se elements. From the position-dependent element percentages shown in Figure 2c, the element contents of Cd and Se increase gradually from the detected positions along the wire, while the element contents of Zn and S are complementary to those of Cd and Se. High-resolution TEM (HRTEM) and corresponding selected area electron diffraction (SAED) investigations further demonstrate that the obtained wires are highly crystallized along their entire lengths (see Figure S1 in the Supporting Information). The above results confirm the formation of these composition gradient ZnCdSSe alloy nanowires.

The PL properties of these composition gradient nanowires were characterized by a dark-field fluorescence microscopy (Axio Imager Z2m, Carl Zeiss) and a point scanning spectrometer (Mapping, HORIBA Jobin Yvon LabRam HR 800). Some ZnCdSSe wires were removed from the as-grown sample and dispersed on a MgF_2 substrate before measurements. Figure 2d gives the dark-field optical micrograph of several dispersed wires under 355 nm laser illumination, which shows the emission colors of all these nanowires gradually changed along their lengths. The red end corresponds to the Cd/Se-rich alloys, and the other

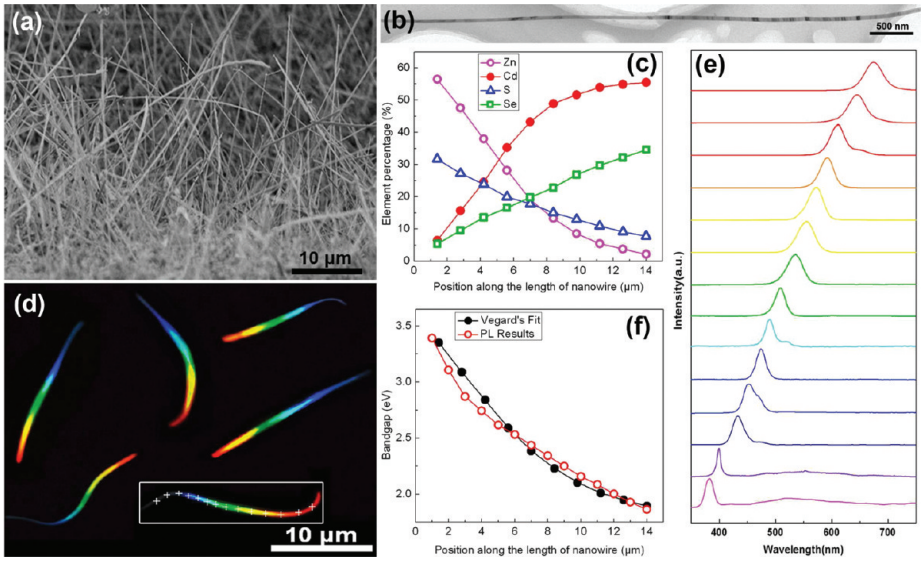

Figure 2. (a) Side-view SEM image of the as-grown sample of full-composition ZnCdSSe nanowires. (b) TEM image of a representative single full-composition wire from the sample. (c) Position-dependent element percentages along the length of the wire for elements Zn, Cd, S, and Se, respectively. (d) The real-color CCD photograph of several dispersed full-composition ZnCdSSe nanowires under a blend of darkfield and 355 nm laser illuminations. (e, f) Position-dependent PL spectra (normalized) and band gap values along the length of a single full-composition wire which is indicated by a white rectangle box in panel d (see the cross marks for the examined points).

dx.doi.org/10.1021/nl203529h |*Nano Lett.* 2011, 11, 5085–5089

gray end corresponds to the Zn/S-rich alloys with a band gap or light emission extended into the ultraviolet (UV) region. The position-dependent photoluminescence (PL) spectra collected along the length of a selected single wire (see the white cross indicted spots in the rectangle box marked wire in Figure 2d) show that every point region has a single-band PL emission, with their peak wavelength gradually changing from ~380 to ~700 nm (see Figure 2e), covering the full visible spectrum range. The local band gap values directly obtained from the PL spectra have good consistency with those calculated from the EDS results combined with Vegard's law for quarternary ZnCdSSe alloys,[38] indicating all of the observed PLs are from the band-edge emission of the band gap graded alloys. The above results demonstrate that full-color band gap graded ZnCdSSe alloy nanowires were achieved by the position/temperature-selected growth that is realized by moving the substrate at a constant speed from the high temperature zone to the low temperature zone within the deposition region.

On the basis of the above substrate moving growth strategy for full-color band gap graded ZnCdSSe nanowires, selected composition control along the wires have been conducted by selectively controlling the positions and moving speed of the substrate during the growth. When the substrate is fixed at a certain position, without any moving during the growth, the obtained nanowires are not composition gradient, having a corresponding position/temperature related constant composition along their whole length. Figure 3a is the real-color picture of the single-color sample grown by keeping the substrate in the fixed position P_1, which shows that the grown wires give almost pure blue light under UV illumination. No apparent color change was observed along the length from the enlarged individual wires (see the lower-right inset in Figure 3a), indicating the grown nanowires are not composition gradient. The in situ PL spectrum of the sample (see the upper-right inset of Figure 3a) gives a single emission band with the peak wavelength centered at 475 nm, which is consistent with the exhibited blue color of the sample. This is reasonable since position P_1 is Zn/S rich, making the grown wires have a wide band gap. If the substrate first stays for some time for growth at position P_1 and then moves quickly to another position P_2 where alloys with a narrower band gap at the "green" region can be deposited for the next growth, the as-grown nanowires should have two main composition distributions and thus have double PL emission bands. Figure 3b gives a real-color picture of such a sample, which shows two main colors (blue and green) along their length. The close-up image of an individual wire as well as the in situ PL spectrum further confirm the double-color emission of these wires. Following the same strategy, tricolor nanowires were achieved by changing three positions of the substrate during growth; i.e., the substrate stays in turn at positions P_1, P_2, and P_3 for growth of blue, green, and red compositions, respectively. The PL images and the corresponding in situ spectra of the achieved tricolor wires are shown in Figure 3c. As expected, the wires have three main color segments along their length, and the PL spectrum contains three emission bands, corresponding to the blue, green, and red segments, respectively. The above results demonstrate that selected composition control along individual wires is feasible through this position/temperature-selected growth strategy. For reference, schematic illustration of the growth process for the composition-selected tricolor wires is shown in Figure 1c.

The ability of realizing selected composition control along the length and especially the growth of tricolor nanowires proves the potential of achieving "white" light nanowires. To achieve nanowires with ideal white light emission, the relative intensity of the emission bands should be well controlled.[2] Since the intensities of the emission bands are determined by the relative length of the corresponding color segments in the wires, the photometric properties of these nanowires can be directly controlled by the respective growth time of these segments. Panels a_1−a_4 of Figure 4 show the real-color paragraphs of some dispersed nanowires under a UV laser illumination removed from four representative tricolor samples (samples T_1−T_4), respectively (see Table S1 in the Supporting Information for the respective growing parameters). The wires in sample T_1 have relatively long blue color segments and short red ones, while in sample T_2 the red segments are much longer than the other two. In sample T_3, the blue color segments are very short compared to the others, and sample T_4 contains wires with comparative length of all three segments. The PL from the nanowire assembles or from a selected wire can be both scanned and collected. Panels b_1−b_4 of Figure 4 show the collected PL spectra for both the nanowire assembles (blue curve) and the selected single wire (red curve) of the four samples, respectively. All spectra are composed of three separate emission bands, with their peak positions having very good correspondence to the blue, green, and red segments in the wires of each sample, respectively. The relative intensities of the three emission bands are also in good proportion to the relative length of the color segments in these samples.

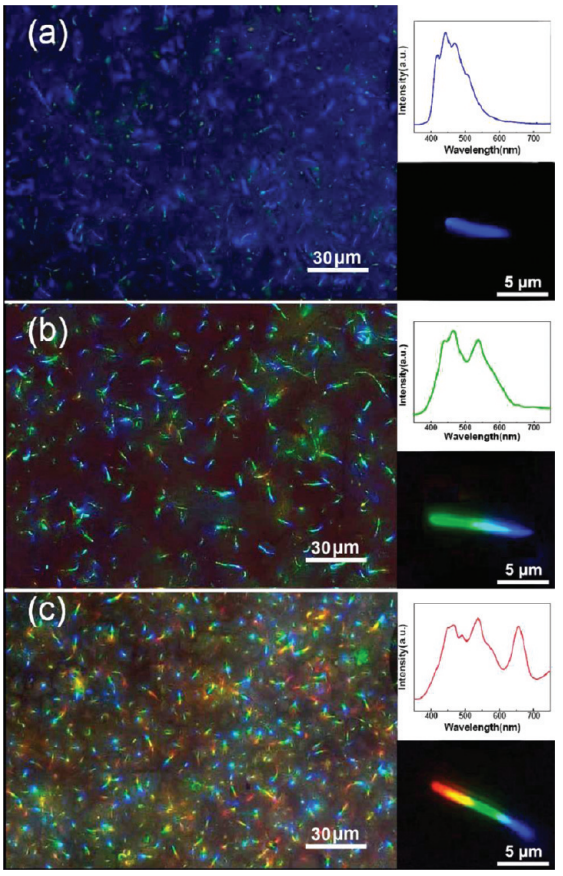

Figure 3. (a−c) Top-view real-color PL photographs of the as-grown single-color (a), double-color (b), and tricolor (c) nanowires, respectively: upper-right insets in each picture, the corresponding in situ collected PL spectrum; lower right-insets in each picture, the enlarged photographs of individual wires.

dx.doi.org/10.1021/nl203529h |*Nano Lett.* 2011, 11, 5085–5089

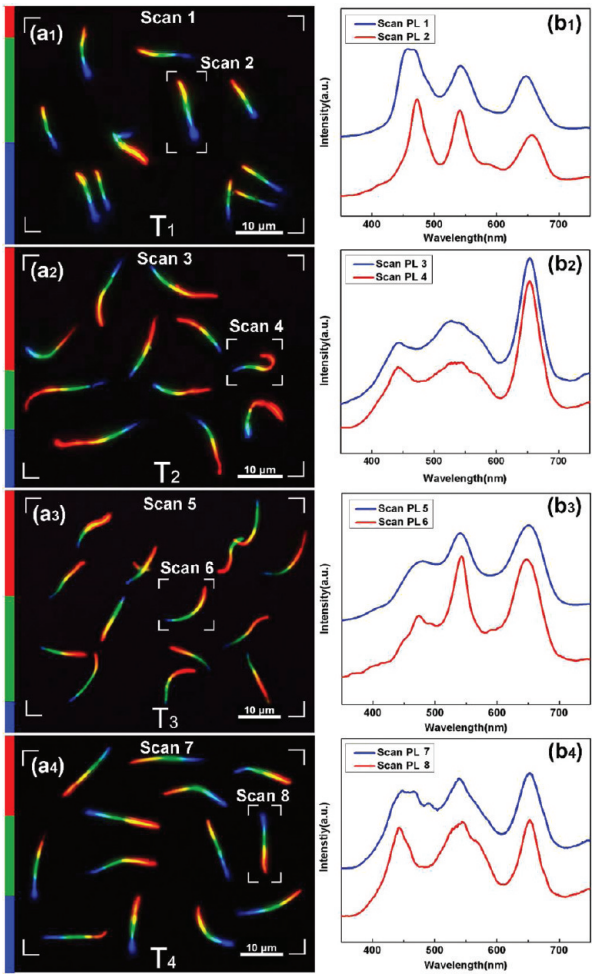

Figure 4. (a_1−a_4) Real-color micrographs of some dispersed nanowires under 355 nm laser illumination removed from four representative tricolor samples (samples T_1−T_4), respectively. (b_1−b_4) The corresponding PL spectra for both the nanowire assembles (blue curve) and the selected single wire (red curve) of the four samples, respectively. The examined nanowire assembles or single wires for PL spectra are indicated in (a_1−a_4), respectively. PL collected using the DuoScan function of a HORIBA Jobin Yvon LabRam HR 800.

More importantly, the spectra of the nanowire assembles are very consistent to the selected single wires in all the examined samples, indicating the composition distribution in the wires of each sample is highly uniform.

The PL photometric properties of these tricolor ZnCdSSe alloy nanowires have been comparatively examined. Panels A_1−A_4 of Figure 5 show the large area micrographs of the dispersed tricolor nanowires under laser illumination removed from the four representative tricolor samples (samples T_1−T_4), respectively. The results show that the PL emissions from samples T_1−T_3 are light blue, light yellow, and orange, respectively, while that from sample T_4 gives a pure white PL emission. The CIE (International Commission on Illumination) chromatic coordinates were calculated using the detected PL spectra shown in panels b_1−b_4 of Figure 4. As shown in Figure 5B, the chromaticity coordinates of samples T_1−T_3 are located at the edge of the white area in the CIE diagram, while that of sample T_4 is located at the center of the white area. The results confirm that only sample T_4 can give pure white

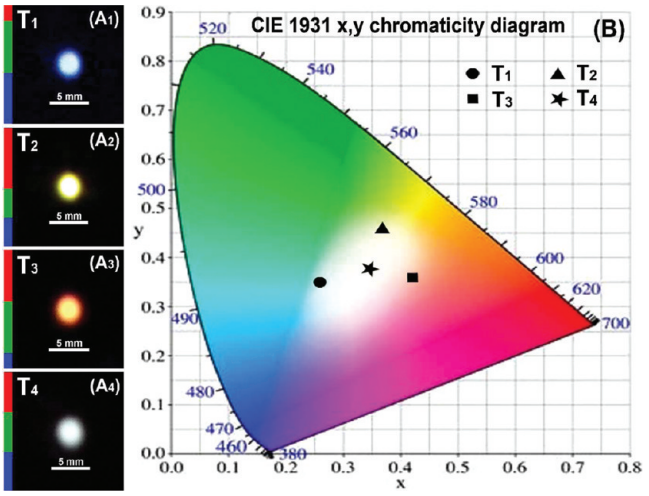

Figure 5. (A_1−A_4) Large area real-color paragraphs of the four representative samples (samples T_1−T_4) under the illumination of a beam of UV light, respectively. (B) CIE chromaticity diagram with the chromatic coordinates of the four representative tricolor samples calculated using the detected PL spectra shown in panels b_1-b_4 of Figure 4, respectively.

light, which is in good agreement with the observations of the real-color PL photographs (Figure 5A_1−A_4).

The spectra of these tricolor ZnCdSSe alloy nanowires are composed of three broad emission subbands, and these subbands cover almost the entire visible region. On the basis of the CRI, the broad band white lighting of these tricolor nanowires should have higher color quality than conventional narrow band white light.[3,39] Moreover, the spatial color mixing of these tricolor nanowires is based on nano/microscale individual wires (see Figure S2 in the Supporting Information), which also help to achieve highly uniform and high-quality white light. At the same time, the semiconductor-based tricolor nanowire white lighting should have competitive conversion efficiency compared to the conventional phosphor-down-conversion white lighting technology.

As for the controllable growth of these tricolor nanowires through the substrate moving strategy, except those main experimental parameters shown in Table S1 (see Supporting Information), some other growth factors should also be taken into account, such as chemical conversion reaction between ZnS and CdSe,[40] thermal conductivity between the substrate and tube, and working temperature of CdSe source. During the growth of the red segment, the pregrown blue segments are exposed in the CdSe vapor with an increasing concentration (P_3) and easily converted into a red one by ion exchange reaction between ZnS and CdSe. Reducing the growth time at P_3 is an effective way to avoid this ion exchange process. The poor thermal conductivity between substrate and the tube could lead to imprecise control of the substrate's temperature during its moving, adding to the difficulty to achieve tricolor nanowires with controllable PL photometric properties. To improve the thermal conductivity between substrate and the tube during the growth, the growth setup was equipped with a cooling system, and this system was turned on at the beginning of the growth. Low working temperature of the CdSe source causes diluted CdSe vapor at P_3 which is not suitable for growth of red segments. However, a too high CdSe vapor concentration accelerates the chemical conversion reaction between ZnS and CdSe. In terms of the working temperature for the CdSe source, 800 °C is the optimal value.

dx.doi.org/10.1021/nl203529h |*Nano Lett.* 2011, 11, 5085–5089

In summary, with temperature-selected composition deposition realized via a substrate moving VLS route, quarternary ZnCdSSe alloy nanowires, with graded band gap covering the entire visible range along their length, were achieved. At the same time, this growth strategy shows the capability to realize composition control by changing the position and moving speed of the substrate during the growth. Representative, tricolor alloy nanowires have been achieved and the photometric properties of these tricolor nanowires are controlled by adjusting the relative lengths of the color segments through carefully modified growth conditions. Finally, on-nanowire white light emission is achieved under optimized growth condition. These band-gap-engineered semiconductor alloy nanowires may find applications in broad band light absorption and emission devices.

■ ASSOCIATED CONTENT

Supporting Information. Figures showing HRTEM and SAED patterns and a tricolor nanowire sample and a table of growth parameters for representative tricolor samples. This material is available free of charge via the Internet at http://pubs.acs.org.

■ AUTHOR INFORMATION

Corresponding Author
*E-mail: (A.-L.P.) Anlian.pan@hnu.edu.cn; (L.-M.T.) phytong@zju.edu.cn.

■ ACKNOWLEDGMENT

The authors thank Professor Charles M. Lieber (Harvard University) for helpful discussions, Dr. Jing Shen and Dr. Suo Ding (HORIBA Jobin Yvon, China) for DuoScan and mapping characterization of nanowires, Dr. Hua Dai (Carl Zeiss, China) for extended focus photographs, Dr.Yu Ye and Professor Lun Dai (Peking University) for part of the spectral measurement. This work is supported by National Natural Science Foundation of China (nos. 61036012, 90923014, and 10974050), the National Basic Research Program of China (Nos. 2007CB307003 and 2012CB932703), and the Hunan Provincial Natural Science Fund (09JJ1009).

■ REFERENCES

(1) Schubert, E. F.; Kim, J. K. *Science* **2005**, *308*, 1274.
(2) Mirhosseini, R; Schubert, M. F.; Chhajed, S.; Cho, J.; Kim, J. K.; Schubert, E. F. *Opt. Express* **2009**, *17*, 10807.
(3) Crawford, M. H. *IEEE J. Sel. Top. Quantum Electron.* **2009**, *15*, 1028.
(4) Nakamura, S.; Pearton, D.; Fasol, G. *The Blue Laser Diode: the complete story*, 2nd ed.; Springer-Verlag: Berlin, 2000.
(5) Tsao, J. Y.; Coltrin, M. E.; Crawford, M. H.; Simmons, J. A. *Proc. IEEE* **2010**, *98*, 1162.
(6) Yan, R. X.; Gargas, D.; Yang, P. D. *Nat. Photonics* **2009**, *3*, 569.
(7) Lieber, C. M.; Wang, Z. L. *MRS Bull.* **2007**, *32*, 99.
(8) Morales, A. M.; Lieber, C. M. *Science* **1998**, *279*, 208.
(9) Könenkamp, R.; Word, R. C.; Schlegel, C. *Appl. Phys. Lett.* **2004**, *85*, 6004.
(10) Chen, C. H.; Chang, S. J.; Chang, S. P.; Li, M. J.; Chen, I. C.; Hsueh, T. J.; Hsu, A. D.; Hsu, C. L. *J. Phys. Chem. C* **2010**, *114*, 12422.
(11) Qian, F.; Li, Y.; Gradecak, S.; Wang, D. L.; Barrelet, C. J.; Lieber, C. M. *Nano Lett.* **2004**, *4*, 1975.
(12) Min, K. W.; Kim, Y. K.; Shin, G.; Jang, S.; Han, M.; Huh, J.; Kim, G. T.; Ha, J. S. *Adv. Funct. Mater.* **2011**, *21*, 119.
(13) Guo, W.; Zhang, M.; Banerjee, A.; Bhattacharya, P. *Nano Lett.* **2010**, *10*, 3355.
(14) Gu, F. X.; Yu, H. K.; Wang, P.; Yang, Z. Y.; Tong, L. M. *ACS Nano* **2010**, *4*, 5332.
(15) Huang, Y.; Duan, X.; Lieber, C. M. *Small* **2005**, *1*, 142.
(16) Seo, K.; Lim, T.; Kim, S.; Park, H. L.; Ju, S. *Nanotechnology* **2010**, *21*, 255201.
(17) Nguyen, H. P. T.; Zhang, S.; Cui, K.; Han, X.; Fathololoumi, S.; Couillard, M.; Botton, G. A.; Mi, Z. *Nano Lett.* **2011**, *11*, 1919.
(18) Lin, H. W.; Lu, Y. J.; Chen, H. Y.; Lee, H. M.; Gwo, S. *Appl. Phys. Lett.* **2010**, *97*, 073101.
(19) Pan, A. L.; Yang, H.; Liu, R. B.; Yu, R. C.; Zou, B. S.; Wang, Z. L. *J. Am. Chem. Soc.* **2005**, *127*, 15692.
(20) Pan, A. L.; Liu, R. B.; Sun, M. H.; Ning, C. Z. *J. Am. Chem. Soc.* **2009**, *131*, 9502.
(21) Pan, A. L.; Wang, X.; He, P.; Zhang, Q.; Wan, Q.; Zacharias, M.; Zhu, X.; Zou, B. S. *Nano Lett.* **2007**, *7*, 2970.
(22) Duan, X. F.; Lieber, C. M. *Adv. Mater.* **2000**, *12*, 298.
(23) Qian, F.; Li, Y.; Gradecak, S.; Park, H.; Dong, Y.; Ding, Y.; Wang, Z. L.; Lieber, C. M. *Nat. Mater.* **2008**, *7*, 701.
(24) Persson, A. I.; Bjork, M. T.; Jeppesen, S.; Wagner, J. B.; Wallenberg, L. R.; Samuelson, L. *Nano Lett.* **2006**, *6*, 403.
(25) Tian, B. Z.; Kempa, T. J.; Lieber, C. M. *Chem. Soc. Rev.* **2009**, *38*, 16.
(26) Gu, F. X.; Yang, Z. Y.; Yu, H. K.; Wang, P.; Tong, L. M.; Pan, A. L. *J. Am. Chem. Soc.* **2011**, *133*, 2037.
(27) Yang, J. E.; Park, W. H.; Kim, C. J.; Kim, Z. H.; Jo, M. H. *Appl. Phys. Lett.* **2008**, *92*, 263111.
(28) Kim, C. J.; Lee, H. S.; Yang, Y. J.; Lee, R. R.; Lee, J. K.; Jo, M. H. *Adv. Mater.* **2011**, *23*, 1025.
(29) Kanungo, P. D.; Wolfsteller, A.; Zakharov, N. D.; Werner, P.; Gosele, U. *Microelectron. J.* **2009**, *40*, 452.
(30) Zakharov, N. D.; Werner, P.; Gerth, G.; Schubert, L.; Sokolov, L.; Gosele, U. *J. Cryst. Growth* **2006**, *290*, 6.
(31) Sirbuly, D. J.; Law, M.; Pauzauskie, P.; Yan, H.; Maslov, A. V.; Knutzen, K.; Ning, C. Z.; Saykally, R. J.; Yang, P. D. *Proc. Natl. Acad. Sci. U.S.A.* **2005**, *102*, 7800.
(32) Dong, A.; Wang, F.; Daulton, T. L.; Buhro, W. E. *Nano Lett.* **2007**, *7*, 1308.
(33) Kim, C. J.; Kang, K.; Woo, Y. S.; Ryu, K. G.; Moon, H.; Kim, J. M.; Zang, D. S.; Jo, M. H. *Adv. Mater.* **2007**, *19*, 3637.
(34) Pan, A. L.; Liu, R. B.; Sun, M. H.; Ning, C. Z. *J. Am. Chem. Soc.* **2009**, *131*, 9502.
(35) Liu, Y.; Zapien, J. A.; Shan, Y. Y.; Geng, C. Y.; Lee, C. S.; Lee, S. T. *Adv. Mater.* **2005**, *17*, 1372.
(36) Pan, A. L.; Zhou, W. C.; Leong, E. S. P.; Liu, R. B.; Chin, A. H.; Zhou, B. S.; Ning, C. Z. *Nano Lett.* **2009**, *9*, 784.
(37) Kuykendall, T.; Ulrich, P.; Aloni, S.; Yang, P. D. *Nat. Mater.* **2007**, *6*, 951.
(38) Pan, A. L.; Liu, R. B.; Sun, M. H.; Ning, C. Z. *ACS Nano* **2010**, *4*, 671.
(39) Ohno, Y. *Proc. SPIE* **2004**, *5530*, 88.
(40) Lee, J. Y.; Kim, D. S.; Park, J. *Chem. Mater.* **2007**, *19*, 4663.